

## ORIGINAL RESEARCH ARTICLE

## Ab Initio Investigation of Gadolinium Zirconate Pyrochlore for Substantial Nuclear Waste Applications

Yahaya Aliyu<sup>1\*</sup>, Nura Ibrahim<sup>1</sup>, Babangida Yahaya<sup>1</sup>, Aliyu Muhammad<sup>1</sup><sup>1</sup>Department of Physics, Faculty of Physical Sciences, Ahmadu Bello University, Zaria, Kaduna, Nigeria.

### ABSTRACT

Nuclear energy is an alternative low CO<sub>2</sub> emission strategy anticipated to mitigate future high energy demand. Radioactive wastes generated from spent nuclear fuel are the major challenge of utilizing nuclear reactors as a source of energy. Pyrochlore compounds are among the rigorous nuclear waste forms considered for High-level waste immobilization. Density functional theory (DFT) based on first-principles simulations was used to study gadolinium zirconate pyrochlore's structural and electronic characteristics (Gd<sub>2</sub>Zr<sub>2</sub>O<sub>7</sub>). The lattice parameters of optimized Gd<sub>2</sub>Zr<sub>2</sub>O<sub>7</sub> are  $\alpha = \beta = \gamma = 60.0^\circ$  and  $a = b = c = 7.635\text{\AA}$ . The conduction band minimum and valence band maximum structure was discovered to be stable and approached the experimental lattice constant. The overlapping of the conduction and valence bands in Gd<sub>2</sub>Zr<sub>2</sub>O<sub>7</sub> indicates its conductive behavior in terms of its electrical characteristics. Due to a usual underestimating of band gap energy in DFT based on electron exchange handling, the estimated band gap energy of 0.09 eV differed from experimental measurements. In addition to band gap energy computation, the computed total density of states and projected density of states show different orbital dominations and energy levels. The findings showed that the Gd<sub>2</sub>Zr<sub>2</sub>O<sub>7</sub> ceramic compound had good resistance to amorphization and could be used for further ab initio investigations.

### ARTICLE HISTORY

Received March 28, 2024.

Accepted June 03, 2024.

Published June 26, 2024.

### KEYWORDS

DFT; High-Level-waste; Gd<sub>2</sub>Zr<sub>2</sub>O<sub>7</sub>; Structural properties, electronic properties

© The authors. This is an Open Access article distributed under the terms of the Creative Commons Attribution 4.0 License (<http://creativecommons.org/licenses/by/4.0>)

### INTRODUCTION

Due to rising energy demands, various alternative energy sources will be needed, including nuclear, solar, and wind power. Consequently, fission and fusion reactions could provide nuclear energy, which has a good potential to meet future energy demands (Kumari *et al.*, 2023). Worldwide, 440 civil nuclear reactors produce over 10% of the world's electricity. Nonetheless, a worldwide problem has been radioactive nuclear waste produced from solid nuclear fuel (SNF), which is mostly made of uranium, thorium, and plutonium. Light water reactors typically produce 30 tons of SNF for every GW produced; this means that over 12,000 tons of SNF and 37,000 metric tons of heavy metal (MTHM) are produced annually. Near the reactor site, these SNF are kept in dry casks or pools (Blackburn *et al.*, 2021; Mir *et al.*, 2021; Wang *et al.*, 2023). High-level waste (HLW) needs to be converted into stable solid forms for safe handling and treatment. Ensuring long-term geological disposal is vital

for preserving the environment and human welfare. Immobilization in extremely chemically resistant glass, ceramic, or glass-ceramic waste forms encapsulates HLW (Blackburn *et al.*, 2021; Panghal *et al.*, 2023). Zirconolite, monazite, fluorapatite, perovskite, and pyrochlore are among the mineral ceramics (SYNROC) that have recently been studied for their potential to dispose of minor actinides (MA) and plutonium (Pu) (Shelyug & Navrotsky, 2021; Shuaibu *et al.*, 2020).

Based on their open structure, pyrochlore compounds with the general formula A<sub>2</sub>B<sub>2</sub>O<sub>7</sub> in which the cations A and B form polyhedral with Oxygen within their crystal structures have been suggested (among SYNROC) as a radionuclides host matrix (Jafar *et al.*, 2021; Li *et al.*, 2023; Nandi *et al.*, 2023). The derivative of the fluorite structure, AO<sub>2</sub> (space group *Fm3m*), is the pyrochlore crystal structure (space group *Fd3m*) (Panghal *et al.*, 2023). Transition metals often occupy the B-site of pyrochlore,

**Correspondence:** Yahaya Aliyu. Department of Physics, Faculty of Physical Sciences, Ahmadu Bello University, Zaria, Nigeria. ✉ [yadabo@abu.edu.ng](mailto:yadabo@abu.edu.ng). Phone Number: +234 806 910 1162.

**How to cite:** Aliyu, Y., Ibrahim, N., Yahaya, B., & Muhammad, A. (2024). Ab Initio Investigation of Gadolinium Zirconate Pyrochlore for Substantial Nuclear Waste Applications. *UMYU Scientifica*, 3(2), 180 – 185. <https://doi.org/10.56919/usci.2432.020>

while rare earth elements typically occupy the A-site. It has been demonstrated that pyrochlore is a dynamic structure that can have an element with different ionic radii occupying both the A and B sites (Finkeldei *et al.*, 2020; Wang *et al.*, 2023). Because of its superiority over other pyrochlore minerals in terms of thermal stability, chemical stability, high radiation resistance, and aqueous durability, zirconate pyrochlore structure ( $A_2Zr_2O_7$ ) has been studied (Li *et al.*, 2023; Nandi *et al.*, 2023; Orlova & Ojovan, 2019; Tang *et al.*, 2023; Zietlow *et al.*, 2017). However, when exposed to radiation damage and self-irradiation, zirconate pyrochlore amorphized (Finkeldei *et al.*, 2020; Finkeldei *et al.*, 2021; Finkeldei, 2015). An amorphization of host nuclear waste form leads to radionuclides release to a biosphere.

Numerous scholarly works employed computational approaches to conduct thorough investigations of pyrochlore compounds (Connor *et al.*, 2021; Ji *et al.*, 2019; Shen *et al.*, 2021; J. Wang *et al.*, 2014). In order to corroborate the experimental results, pyrochlore's damage cascade creation, defect formation energy, and order-disorder transitions have all been computationally investigated. Density functional theory (DFT) has recently proven to be an excellent method for simulating enthalpies of formation (Finkeldei *et al.*, 2020; Shuaibu *et al.*, 2020; Tanti & Kaltsoyannis, 2021). By using Density Functional Theory (DFT) calculations, this paper seeks to present a thorough analysis of the structural and electrical characteristics of gadolinium zirconate pyrochlore.

## MATERIALS AND METHODS

Quantum Espresso is used for all computations (QE). The Perdew-Burke-Ernzerhof (PBE) functional was used to characterize the exchange-correlation potential when the generalized gradient approximation (GGA) was used (Shuaibu *et al.*, 2020). To achieve successful convergence sampling in the Brillouin zone (BZ) integration, an  $8 \times 8 \times 8$  Monkhost Pack k-points mesh was utilized (Idris *et al.*, 2020; Lawal *et al.*, 2018). For the electron wave function expansion, kinetic energy cutoffs of 50 Ry connected to the plane-wave basis set were employed. The atomic locations, sizes, and shapes that make up the supercell geometry were loosened to fewer than  $10^{-3}$  eV/Å of Hellmann-Feynman forces on each ion. The 88-atom supercell of the cubic structure of  $Gd_2Zr_2O_7$  was used for the computations.

## RESULTS AND DISCUSSION

### Structural Properties of Gadolinium Zirconate Pyrochlore Compound

As seen in Figure 1, pyrochlore ( $Gd_2Zr_2O_7$ ) is made up of corner-linked layers of  $Gd_2O_3$  and  $Zr_2O_3$ . In this work, the cubic (FCC lattice) crystal structure associated with the

primitive unit cell was utilized. A  $2 \times 2 \times 2$  supercell makes up the supercell. The supercell is made up of 88 atoms, of which 16 are Gd, 16 are Zr, and 56 are O. A regular cubic that is connected to one another inside shared edges is created when four O atoms enhance each Gd atom, and each Zr atom is enriched by four O atoms. The supercell's optimized crystal parameters are  $a = b = c = 7.635 \text{ \AA}$  and  $\alpha = \beta = \gamma = 60.0^\circ$ , which are less than the  $a_0 = 10.472 \text{ \AA}$  experimental lattice constant (Zhang *et al.*, 2017).

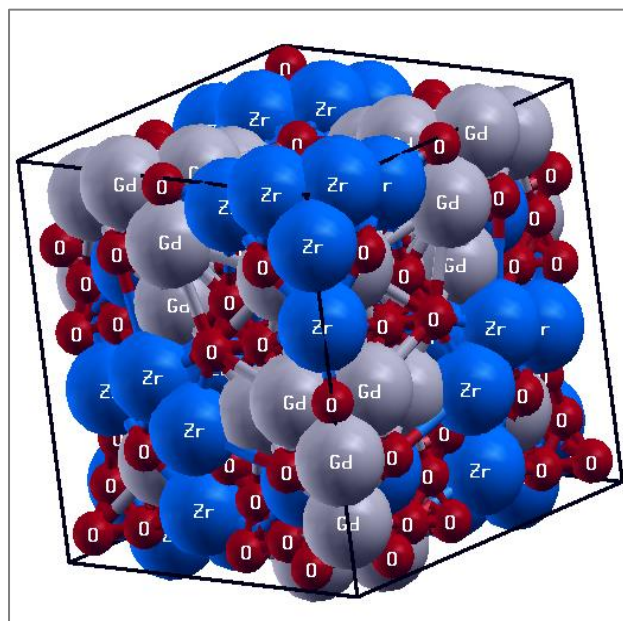


Figure 1 depicts the bulk structure of a simulated cubic Gadolinium Zirconate Pyrochlore ( $Gd_2Zr_2O_7$ ). Oxygen ions are represented by red (small, dark) spheres, Zr ions by blue (big, grey) spheres, and Gd ions by cyan (large, cyan) spheres.

### Electronic Properties of Gadolinium Zirconate Pyrochlore ( $Gd_2Zr_2O_7$ )

Calculating a solid's electronic properties, such as its band structure, density of state (DOS), projected density of state (PDOS), and charge density distributions, is essential to understanding its electronic structure (Radzwan *et al.*, 2020).

#### Band Structure of Pyrochlore Compound ( $Gd_2Zr_2O_7$ )

Using PBE-GGA, Figure 2(a) displays the electronic band structure of gadolinium zirconate pyrochlore ( $Gd_2Zr_2O_7$ ). The band structure energy is displayed between -2.00 eV and 2.0 eV, with 11 high symmetry locations ( $\Gamma$ -X-W-K- $\Gamma$ ) chosen. The zero (0 eV) on the energy scale represents the Fermi level of the crystal band structure. Because of the small energy band gap between the valence and conduction bands, the overlapping valence band maximum (VBM) and conduction band minimum (CBM)

at the Fermi level show that  $Gd_2Zr_2O_7$  is conductive. The material's predicted band gap energy is 0.09 eV, which differs from the 3.02 eV experimental result (Perenlei *et al.*, 2015) as well as additional computed results resulting from the well-acknowledged underestimating of the band gap caused by incorrect treatment of the electron-exchange in

standard DFT (Chiromawa *et al.*, 2020; Shein *et al.*, 2022) and applications of different and modified pseudopotential. Hence, in the valence band, electrons predominate in the energy range of -2eV to 0eV, followed by a conduction state from 0eV to 2eV.

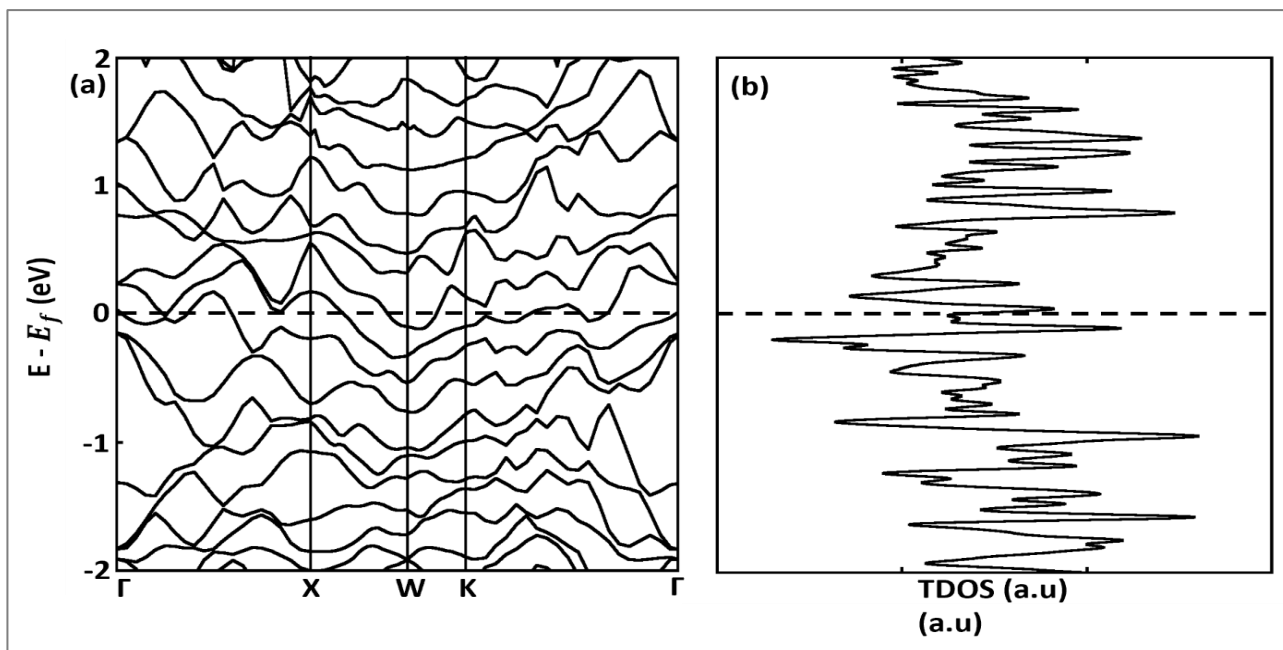


Figure 2. Band Structure (a) and Total Density of state (b) of Pyrochlore ( $Gd_2Zr_2O_7$ ) compound.

#### Density of State (DOS) and Projected Density of State (PDOS) for Pyrochlore Compound ( $Gd_2Zr_2O_7$ )

The overall density of state (DOS), projected density of state (PDOS), and charge density distribution of pyrochlore were examined to better understand the nature of the energy gap. While the orbital dominations are explained by PDOS, the DOS plot described the number of states per energy level present for the occupation of the  $Gd_2Zr_2O_7$  molecule. Figure 2b shows that the peaks at the valence band and conduction band of the entire DOS are nearly identical. The Gd-5s, Zr-4s, and O-2s orbitals contributed to the lowest occurrence of the valence band, the highest peak, which occurred between -4 eV and -1 eV in pyrochlore. The Gd-5p, Zr-4p, and O-2p orbitals dominated the intermediate occurrence of the valence band, which occurred between -1 eV and 1.0 eV. The lowest peak, which dominates the Gd-5d, Zr-4d, and O-2p orbitals, is the highest occurrence of the valence band, which is located just below the Fermi level between 2 eV and 4 eV (Figure 3). According to Raza *et al.* (2022), the high number of states close to the Fermi levels exhibits metallic behavior with respect to the density of states.

#### The Charge Density Plots for Pyrochlore Compound ( $Gd_2Zr_2O_7$ )

The electronic charge density in the crystallographic plane is displayed to get a comprehensive image of the entire electronic charge distribution of the pyrochlore ( $Gd_2Zr_2O_7$ ). It clarifies the nature of charge transfer between anions and cations and chemical bonding. Figure 4 illustrates how charge transfer between atoms is indicated by the spherical form of charge around the cations ( $Gd^{2+}$ ,  $Zr^{4+}$ ). According to the thermometer in Figure 4, the maximum charge buildup is associated with the magenta color, which creates the highest charge (+2.1612). Hence, the zirconium (4s) atom has the largest charge distribution compared to other atoms. Titanium has a considerable charge density, whereas the red-colored Oxygen (2s) atom has a lesser charge density (+0.2539). Figure 4 illustrates that  $Gd_2Zr_2O_7$  contains an ionic bond, a sign of strong resistance to amorphization. Because of the high concentration of zirconium atoms, pyrochlores containing zirconium atoms are typically naturally ionic (Raza *et al.*, 2022).



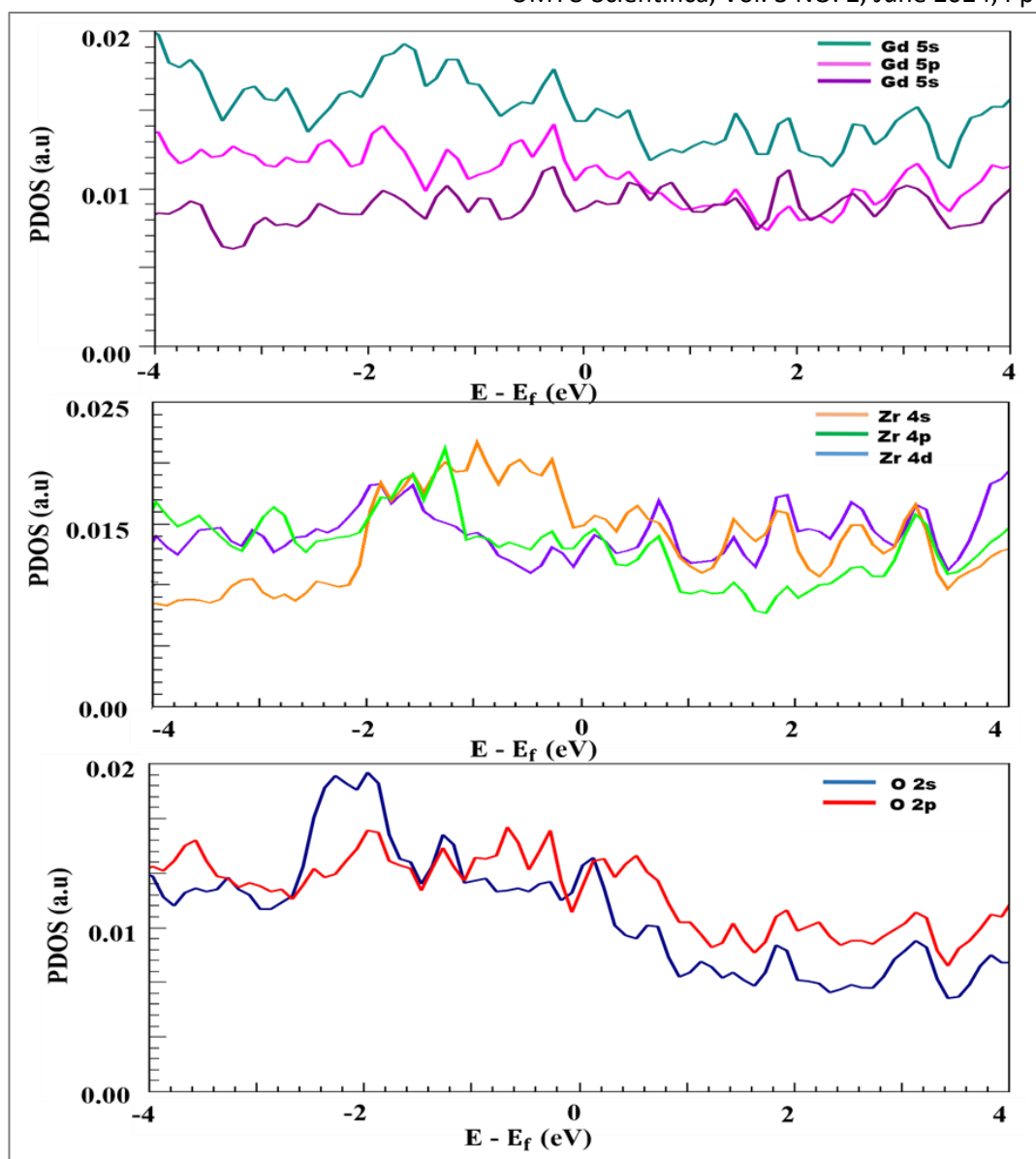


Figure 3. Partial Density of State (PDOS) for Pyrochlore ( $Gd_2Zr_2O_7$ ) Compound.

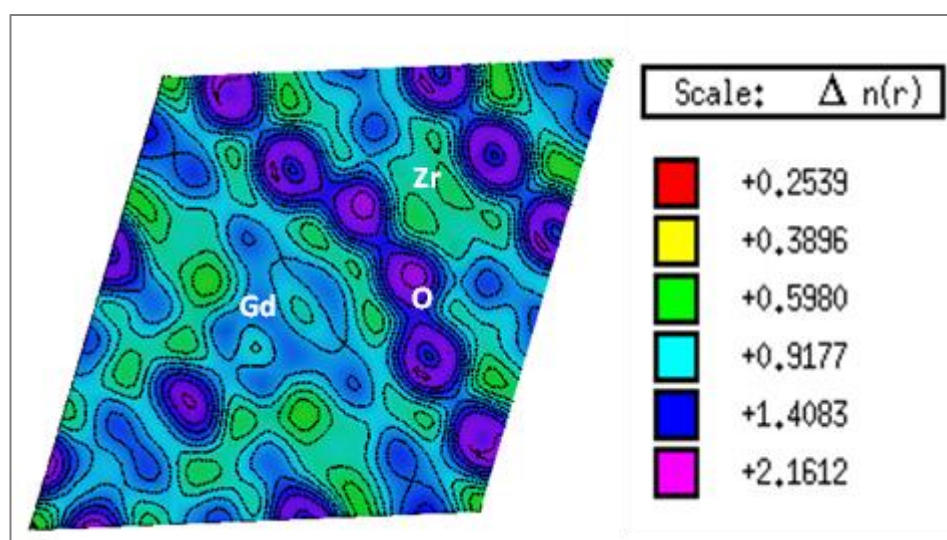


Figure 4 shows the front view of the Pyrochlore scale's charge density distribution plot (also known as an electronic contour graph), which shows ranges of the same density values in atomic units (a.u.).

## CONCLUSION

This work uses the Quantum Espresso (QE) code to implement a thorough investigation based on the density functional theory and generalized gradient approximations. The investigation explores the impact of structural and electronic properties on the radiation resistance of Gadolinium zirconate Pyrochlore ( $Gd_2Zr_2O_7$ ), a potential ceramic for immobilizing nuclear waste. The  $Gd_2Zr_2O_7$  crystal structure was discovered to be stable and close to the outcomes of computations and experiments. The overlapping Conduction Band Minimum (CBM) and Valence Band Maximum (VBM) in the electronic characteristics of  $Gd_2Zr_2O_7$  showed the material's conductivity due to DFT's underestimating of the band gap energy, a band gap energy of 0.09 eV, which differs from experimental and prior computed results.

Moreover, the band gap energy estimates are consistent with the total of state (DOS) and projected density of state calculations, indicating different numbers of states per energy level and orbital dominance between CBM and VBM. The  $Gd_2Zr_2O_7$  molecule and zirconium with the largest charge distribution exhibit an ionic bond nature according to the charge density distribution. The findings showed that the  $Gd_2Zr_2O_7$  ceramic compound had good resistance to amorphization. The findings imply the feasible application of Quantum Espresso (QE) code to interpret nuclear materials' physical and chemical properties. The finding could be used to predict further thermal and chemical properties of zirconate pyrochlore (basis) based on ab initio studies. Further analysis could be carried out to investigate further the effect of doping zirconate pyrochlore compound with actinides

## ACKNOWLEDGMENTS

We appreciate the thoughtful comments and explanations from the co-authors.

## DECLARATION OF COMPETING INTEREST

The authors have no conflicting or private interests.

## REFERENCES

Blackburn, L. R., Bailey, D. J., Sun, S. K., Gardner, L. J., Stennett, M. C., Corkhill, C. L., & Hyatt, N. C. (2021). Review of zirconolite crystal chemistry and aqueous durability. *Advances in Applied Ceramics*, 120(2), 69–83. [\[Crossref\]](#)

Chiromawa, I. M., Shaari, A., Razali, R., Taura, L. S., & Lawal, A. (2020). Structural stabilities, electronic structure, optical and elastic properties of ternary  $Fe_2SiO_4$  spinel: An ab initio study. *Materials Today Communications*, 25(September), 101665. [\[Crossref\]](#)

Connor, T., Cheong, O., Bornhake, T., Shad, A. C., Tesch, R., Sun, M., He, Z., Bukayemsky, A., & Vinograd, V. L. (2021). *Pyrochlore Compounds From Atomistic Simulations*. 9(November), 1–14. [\[Crossref\]](#)

Finkeldei, S., Stennett, M. C., Kowalski, P. M., Ji, Y., De

Visser-Týnová, E., Hyatt, N. C., Bosbach, D., & Brandt, F. (2020). Insights into the fabrication and structure of plutonium pyrochlores. *Journal of Materials Chemistry A*, 8(5), 2387–2403. [\[Crossref\]](#)

Finkeldei, Sarah C., Chang, S., Ionescu, M., Oldfield, D., Davis, J., Lumpkin, G. R., Simeone, D., Avdeev, M., Brandt, F., Bosbach, D., Klinkenberg, M., & Thorogood, G. J. (2021). Insight Into Disorder, Stress and Strain of Radiation Damaged Pyrochlores: A Possible Mechanism for the Appearance of Defect Fluorite. *Frontiers in Chemistry*, 9(November), 1–20. [\[Crossref\]](#)

Finkeldei, Sarah Charlotte. (2015). *Pyrochlore as nuclear waste form: Actinide uptake and chemical stability* (Vol. 276). [www.iaea.org](http://www.iaea.org)

Idris, M. C., Shaari, A., Razali, R., Lawal, A., & Ahams, S. T. (2020). DFT+U studies of structure and optoelectronic properties of  $Fe_2SiO_4$  spinel. *Computational Condensed Matter*, 23, e00460. [\[Crossref\]](#)

Jafar, M., Phapale, S. B., Nigam, S., Achary, S. N., Mishra, R., Majumder, C., & Tyagi, A. K. (2021). The implication of aliovalent cation substitution on the structural and thermodynamic stability of  $Gd_2Ti_2O_7$ : Experimental and theoretical investigations. *Journal of Alloys and Compounds*, 859(xxxx), 157781. [\[Crossref\]](#)

Ji, Y., Marks, N. A., Bosbach, D., & Kowalski, P. M. (2019). Elastic and thermal parameters of lanthanide-orthophosphate ( $LnPO_4$ ) ceramics from atomistic simulations. *Journal of the European Ceramic Society*, 39(14), 4264–4274. [\[Crossref\]](#)

Kumari, R., Pathak, N., Saini, M., Parambil, K., Ranjan, M., & Lata, C. (2023). *Synthesis of the chemically durable glass-ceramic matrix for radioactive waste immobilisation*. October 2022, 1–8.

Lawal, A., Shaari, A., Ahmed, R., & Taura, L. S. (2018). Investigation of excitonic states effects on optoelectronic properties of  $Sb_2Se_3$  crystal for broadband photo-detector by highly accurate first-principles approach. *Current Applied Physics*, 18(5), 567–575. [\[Crossref\]](#)

Li, Y., Lei, Y., Zhao, S., Xiao, H., Liu, H., Wang, Y., Luo, Y., Zhang, J., Wang, J., Ewing, R. C., & Wang, C. (2023). *Scripta Materialia Phase transformation and radiation resistance of B-site high entropy pyrochlores*. 229(November 2022), 1–6. [\[Crossref\]](#)

Mir, A. H., Hyatt, N. C., & Donnelly, S. E. (2021). An in-situ TEM study into the role of disorder, temperature and ballistic collisions on the accumulation of helium bubbles and voids in glass-ceramic composites. *Journal of Nuclear Materials*, 548(January). [\[Crossref\]](#)

Nandi, C., Phatak, R., Kesari, S., Shafeeq, M., Patkare, G., Jha, S. N., Rao, R., Mishra, S., Prakash, A., & Behere, P. G. (2023). *Influence of synthesis atmosphere on the solid solubility of uranium at B-site of  $Nd_2Zr_2O_7$  pyrochlore*. 574. [\[Crossref\]](#)

Orlova, A. I., & Ojovan, M. I. (2019). Ceramic mineral

- waste forms for nuclear waste immobilization. *Materials*, 12(16). [\[Crossref\]](#)
- Panghal, A., Kumar, Y., Singh, F., & Singh, N. L. (2023). Role of structural ordering on the radiation response of  $Gd_2Zr_2O_7$  pyrochlore. 49(March 2022), 12191–12200. [\[Crossref\]](#)
- Perenlei, G., Alarco, J. A., Talbot, P. C., & Martens, W. N. (2015). Synthesis, Characterization, and Electronic Structure Studies of Cubic  $Bi_{1.5}ZnTa_{1.5}O_7$  for Photocatalytic Applications. *International Journal of Photoenergy*, 2015. [\[Crossref\]](#)
- Radzwan, A., Ahmed, R., Shaari, A., & Lawal, A. (2020). First-principles study of electronic and optical properties of antimony sulphide thin film. *Optik*, 202(October 2019). [\[Crossref\]](#)
- Raza, A., Afaq, A., Kiani, M. S., Ahmed, M., Bakar, A., & Asif, M. (2022). First-principles calculations to investigate elasto-mechanical and optoelectronic properties of pyrochlore oxides  $X_2Zr_2O_7$  ( $X = \frac{1}{4}La, Nd$ ). [\[Crossref\]](#)
- Shein, I. R., Vlasov, M. I., & Piiir, I. V. (2022). Effect of Li and Li-RE co-doping on structure, stability, optical and electrical properties of bismuth magnesium niobate pyrochlore. 145. [\[Crossref\]](#)
- Shelyug, A., & Navrotsky, A. (2021). Thermodynamics of Fluorite-Structured Oxides Relevant to Nuclear Energy: A Review. *ACS Earth and Space Chemistry*, 5(3), 703–721. [\[Crossref\]](#)
- Shen, H., Li, M., Li, P., Xiao, H., Zhang, H., & Zu, X. (2021). Defect formation and its effect on the thermodynamic properties of  $Pu_2Zr_2O_7$  pyrochlore: a first-principles study. *Journal of the American Ceramic Society*, 104(5), 2301–2312. [\[Crossref\]](#)
- Shuaibu, A., Abdu, S., Aliyu, Y., & Kauru, Y. A. (2020). An Investigation of Structural and Electronic Properties of Zirconolite ( $CaZrTi_2O_7$ ) Using Density Functional Theory. *FUW Trends in Science & Technology Journal*, 5(3), 943–947.
- Tang, Y., Wang, J., Wang, J., Wang, Y., & Li, X. (2023). Order-disorder structural transition of  $Nd_2(Zr_{1-x}Ce_x)_2O_7$  pyrochlores prepared by auto-combustion method. 2(November 2022), 2–9. [\[Crossref\]](#)
- Tanti, J., & Kaltsoyannis, N. (2021). Computational study of the substitution of early actinides and Ce into zirconolite. *Journal of Nuclear Materials*, 543, 152525. [\[Crossref\]](#)
- Wang, J., Ewing, R. C., & Becker, U. (2014). Defect formation energy in pyrochlore: The effect of crystal size. *Materials Research Express*, 1(3). [\[Crossref\]](#)
- Wang, Y., Jing, C., Ding, Z., Zhang, Y., Wei, T., Ouyang, J., Liu, Z., Wang, Y., & Wang, Y. (2023). The Structure, Property, and Ion Irradiation Effects of Pyrochlores: A Comprehensive Review. [\[Crossref\]](#)
- Wang, Z., Zhu, C., Wang, H., Wang, M., Liu, C., Yang, D., & Li, Y. (2023). Preparation and irradiation stability of  $A_2B_2O_7$  pyrochlore high-entropy ceramic for immobilization of high-level nuclear waste. 574. [\[Crossref\]](#)
- Zhang, S., Zhang, H. B., Zhao, F. A., Jiang, M., Xiao, H. Y., Liu, Z. J., & Zu, X. T. (2017). Impact of isovalent and aliovalent substitution on the mechanical and thermal properties of  $Gd_2Zr_2O_7$ . 7(June), 1–13. [\[Crossref\]](#)
- Zietlow, P., Beirau, T., Mihailova, B., Groat, L. A., Chudy, T., Shelyug, A., Navrotsky, A., Ewing, R. C., Schlüter, J., Škoda, R., & Bismayer, U. (2017). Thermal annealing of natural, radiation-damaged pyrochlore. *Zeitschrift Fur Kristallographie - Crystalline Materials*, 232(1–3), 25–38. [\[Crossref\]](#)